Published in final edited form as:
J Biomed Mater Res A. 2011 April ; 97(1): 93–102. doi:10.1002/jbm.a.33034.

Directed assembly of cell-laden microgels for building porous three-dimensional tissue constructs

Fumiki Yanagawa[a,b,1], **Hirokazu Kaji**[a,b,c,1], **Yun-Ho Jang**[a,b], **Hojae Bae**[a,b], **Du Yanan**[a,b], **Junji Fukuda**[a,b,d], **Hao Qi**[a,b], and **Ali Khademhosseini**[a,b,*]

[a]Center for Biomedical Engineering, Department of Medicine, Brigham and Women's Hospital, Harvard Medical School, Cambridge, MA 02139, USA

[b]Harvard-MIT Division of Health Sciences and Technology, Massachusetts Institute of Technology, Cambridge, MA 02139, USA

[c]Department of Bioengineering and Robotics, Graduate School of Engineering, Tohoku University, 6-6-01 Aramaki, Aoba-ku, Sendai 980-8579, Japan

[d]Graduate School of Pure and Applied Sciences, University of Tsukuba, 1-1-1 Tennodai, Tsukuba, Ibaraki 305-8573, Japan

Abstract

The organization of cells within a well-defined microenvironment is important in generating the resulting tissue function. However, the cellular organization within biodegradable scaffolds often does not resemble those of native tissues. In this study, we present directed assembly of microgels to organize cells for building porous 3D tissue constructs. Cell-laden microgels were generated by molding photocrosslinkable polyethylene glycol diacrylate (PEGDA) within a poly(dimethyl siloxane) (PDMS) stencil. The resulting microgels were subsequently packed as individual layers (1 mm in height) on a glass substrate by removing the excess pre-polymer solution around the microgels. These clusters were crosslinked and stacked on one another to fabricate thick 3D constructs that were greater than 1 cm in width and 3 mm in thickness. To generate pores within the engineered structures, sodium alginate microgels were integrated in the engineered constructs and used as a sacrificial template. These pores may be potentially useful for fabricating a vascular network to supply oxygen and nutrients to the engineered tissue constructs. This simple and versatile building approach may be a useful tool for various 3D tissue culture and engineering applications.

Keywords

Microgels; directed assembly; poly(ethylene glycol) diacrylate; sodium alginate; oxygen diffusion

[*]Corresponding author: Ali Khademhosseini, (alik@rics.bwh.harvard.edu) Partners Research Building, Rm 252, 65 Landsdowne Street Cambridge MA, USA 02139 Tel: 617-768-8395; Fax: 617-768-8477.
[1]These authors contributed equally to this work

Introduction

There is a severe shortage of tissues that can be used to repair diseased or defective tissues. Recently, tissue engineering has emerged to fabricate tissues in sufficient quantities to repair defective tissues1. Over the past few decades, many examples have been introduced that utilize biodegradable porous scaffolds to engineer tissues and few of them have been applied in the clinical trials1–2. While this approach has been shown to be useful3–8, the precise control over the arrangement of cells as well as the structure and composition of microenvironment, crucial factors maintaining the tissue structure and function, remains to be solved9.

To engineer tissues with biomimetic architecture and function, “bottom-up” (also known as “modular”) tissue engineering has emerged which aims to recreate the tissue architecture by engineering individual microgel blocks with unique microstructural features and assembling these blocks into larger engineered tissues10. Several techniques to engineer these tissues have been developed such as random assembly11, manual manipulation12, multi-layer photopatterning13, and microfluidic-directed assembly14. Random assembly of microgel blocks is rapid and simple, but lacks the control over the final structure of the hydrogel aggregate. Manual manipulations may provide the proper control of microgel block assembly, but this approach is relatively slow and non-scalable for fabrication of large tissues. Multilayer photopatterning and microfluidic-directed assembly can also be used to create highly sophisticated microgel assembly architectures, but long operational times and complex equipments are usually required.

Directed assembly of cell-laden microgels to build tissue-like constructs with defined microarchitectures is another method used to assemble microgel blocks15. The advantages of directed assembly technique include the ability to recapitulate the native architecture of natural repeated units of tissues, such as lobule of the liver13, without the need for complicated equipments and manipulations. A recent work in this area has shown the fabrication of centimeter scale cell-laden microgel assemblies at the liquid-air interface of hydrophobic solutions16. These directed assembly techniques at the two-phase interface is powerful tool for generating tissue-like constructs, but the capillary forces at the interface of two-phase limit the movement of the microgel units on the hydrophobic solution17. In addition, these constructs lack the spaces for adequate supply of oxygen, nutrients, and other soluble factors necessary for the cell survival for fabrication of thicker and more complicated 3D constructs. Therefore, the development of assembly technique supporting controlled allocation of cells and spaces to improve medium flow may be required for building thick 3D tissue constructs.

The objective of this study was to develop a directed assembly technique for generating 3D tissue-like constructs with engineered pores. To achieve this objective, we developed a three step approach that involved microgel fabrication, 2D assembly of microgels to form sheets, and layer-by-layer stacking of assembled 2D sheets. To generate porosity within the 3D construct, we used sodium alginate as a sacrificial microgel block which can be selectively dissolved after the assembly step.

Materials and methods

Materials

All reagents were purchased from Sigma-Aldrich, unless specifically mentioned otherwise.

Fabrication of PDMS stencil

PDMS stencils were fabricated by curing a layer of PDMS on a silicon wafer patterned with a negative photoresist (SU-8 2150, Microchem, Newton, MA). Photomasks with hexagonal patterns that were either 720 μm or 900 μm in width respectively were designed by using AutoCAD software and printed on transparencies with 20,000 dpi resolution (CAD/Art Services, Inc., Bandon, OR). Master molds containing the 1 mm thick hexagonal patterns were then fabricated by patterning the negative photoresist on a 4-inch silicon wafer. About 10 mL of the photoresist was dispensed on the wafer, which was spin-coated at 500 rpm for 35 sec. The wafer was then baked on a hot plate at 95 °C for 8 h to remove the solvent in the photoresist. The designed patterns were transferred by exposure to UV light at 2160 mJ/cm^2, and then the wafer was cured on a hot plate at 95 °C for 50 min. Finally, the unexposed area of the photoresist was developed in PM acetate for 40 min by immersion with agitation. PDMS stencils were fabricated by mixing silicone elastomer and curing agent (Sylgard 184, Essex Chemical, Midland, MI) at a 10:1 ratio and pouring the PDMS pre-polymer on the silicon master. Excess PDMS on top of the SU-8 structures was scraped away and the wafer was then cured at 80 °C for 2 h and the PDMS stencils were peeled off the silicon wafer. During the silicon mold fabrication, the thickness of the ultra-thick photoresist depends on the dispensed volume as well as a spin speed18. The calculated volume to form 1 mm thick photoresist inside 4” circular wafer is 7.85 mL; however we dispensed 10 mL to ensure complete coverage and compensate for the loss of resist during the process. By using this approach, we could obtain 1 mm thick SU-8 molds which resulted in 1 mm thick PDMS stencil.

Photolithographic fabrication of microgels

PEGDA microgels of controlled shapes and sizes were fabricated by using photolithography (Fig. 1A). Pre-polymer solution was prepared by dissolving 0.5% photoinitiator (wt/wt), 2-hydroxy-1-(4-(hydroxyethoxy)phenyl)-2-methyl-1-propanone (Irgacure 2959; CIBA Chemicals), and 20% (w/w) PEGDA (M_w 1,000 Da; Sigma) in Dulbecco’s Phosphate Buffered Saline (DPBS; GIBCO). To mix the contents, the solution was stirred at 80°C for 30 min. A drop containing 30 μL of the photocrosslinkable PEGDA pre-polymer and photoinitiator was pipetted onto an 18 × 18 mm PDMS stencil with hexagonal patterns after the PDMS was attached on the glass slide (25 × 25 mm). Another glass slide was then placed on top of the solution drop, which created an evenly distributed film of pre-polymer solution between the two glass slides. Subsequently, microgels were formed by exposing the pre-polymer solution to UV light (360–480 nm; 12.4 mW/cm^2). The UV light was irradiated to the system from various directions (top, top and bottom, top and bottom and 4 sides, see Fig. 2C), while maintaining the total exposure time was 28 sec. To label individual microgels, rhodamine-dextran (M_w = 10 kDa) was mixed with pre-polymer solution at a concentration of 0.2 mM before photocrosslinking.

Microgels assembly on the glass slide surface and secondary crosslinking

To harvest the microgels, the top glass slide and the PDMS stencil were carefully removed (Fig. 1A). To direct the assembly and compaction on the surface of the glass slide, 20 μL of the pre-polymer solution was added to seventy microgels and removed by a pipette and an absorbent material (e.g., tissue paper), which ensured that only pre-polymer entrapped between the units remained. Also, a small agitation was applied to the entire system to reduce the local defects and overlapping of the microgels. Microgel assemblies formed on the slide were exposed to secondary UV crosslinking for 6 sec from the top, bottom, and sides.

Fabrication and dissolution of alginate microgels as a sacrificial material

Alginate microgels19–20 were fabricated by using a PDMS stencil (Fig. 1B). Sodium alginate was dissolved in 0.9 wt% NaCl at a concentration of 2.0% w/v and then stirred for 24 h. The suspension was immediately poured into the hexagonal patterned PDMS stencil (dimensions: 900 μm in width × 1000 μm in height) and excess alginate was removed by gently wiping the stencil. Then, the stencil was immediately immersed in a solution of 100 mM $CaCl_2$. To label individual microgels, green fluorescent microbeads (1% solid, D = 5 μm; Duke Scientific) was mixed with the suspension solution before crosslinking.

To direct the assembly of microgels of PEGDA and alginate, the procedure mentioned in the above section was conducted after the alginate microgels were added to the PEGDA microgels at a ratio of 15%. To elute sodium alginate microgel units, the assembled microgels were immersed in NaCl solution containing 5.0% w/v sodium triphosphate (TPP) for 90 min at room temperature.

Fabrication of 3D multilayered constructs

To fabricate the 3D constructs, individual microgel cluster layers with or without pores were stacked in a layer-by-layer manner on a glass slide with 20 μL of pre-polymer solution added between each layer (Fig. 1C). Pre-polymer solution was removed by a pipette and an absorbent material, which ensured that only pre-polymer entrapped between the layers remained. In our experiments we repeated this process three times to generate constructs with three layers of the microgel layers. To stabilize the assembled units, construct formed on the slides were exposed to UV crosslinking for 6 sec from beside.

Fabrication and assembly of cell-laden microgels

Mouse fibroblast (NIH-3T3) and hepatocarcinoma cells (HepG2) were maintained in DMEM supplemented with 10% fetal bovine serum in a 5% CO_2 humidified incubator at 37 °C. To encapsulate cells in the pre-polymer solution, the cells were harvested by using 1% (NIH-3T3) or 3% (HepG2) trypsin and resuspended in the pre-polymer solution at a concentration of $1 \times 10^6 – 2 \times 10^7$ cells / mL. Cell-laden microgel assemblies were generated according to the conditions in the above-mentioned experiments. These constructs were maintained in DMEM supplemented with 10% FBS and 1% Penicillin-Streptomycin in an incubator at 37 °C and a 5% CO_2 atmosphere for 24 h after fabrication, while the culture dish was kept shaking at 130 rpm. Cell viability was characterized by incubating cells with live/dead (EthD-1/Calcein) assay kit (1.0 μL of ethidium homodimer-1 and 4.0 μL of

Calcein AM; Molecular Probes) in 6.0 mL of the culture medium for 3 h, followed by wash with DPBS. Cells were labeled green with Calcein (live) or red with EthD-1 (dead). Cell viability was determined from the live/dead images using NIH Image software. As it was difficult in some cases to distinguish individual cells in the constructs, areas of green and red were analyzed to obtain the viability.

Statistical Analysis

Data from at least three independent experiments were analyzed and values were represented as mean ± standard deviation of means. The Student t-test was used to analyze the statistical significance of the data. Values with a P-value less than 0.05 were considered statistically significant.

Results and discussion

Fabrication and evaluation of PEGDA microgels

Figure 1 shows a schematic diagram of the directed microgel assembly process, which can be summarized by the following three steps (Figure 1A–C): (1) fabricating PEGDA / alginate microgels by using PDMS stencils; (2) directing the assembly of the microgels to fabricate assembled monolayer on a glass slide; (3) layer-by-layer stacking of individual monolayers.

PEGDA microgels were fabricated by using a PDMS stencil containing an array of hexagonal holes. Figure 2A shows a top-view microscopic image of PEGDA microgels after retrieval from the PDMS stencil. As it can be seen PEGDA microgels were generated in a uniform manner. However, when viewed from the side, it was found that the shape of the microgels varied by the direction of the UV irradiation to the PDMS stencil containing the pre-polymer solution. Figure 2B shows the typical shape of the microgels when the UV was irradiated from various directions (see Fig. 2C). To estimate the influence of the UV direction on the side of PEGDA microgel geometry, the gap between maximum and minimum width of a microgel were evaluated. This gap decreased significantly when the pre-polymer solution was irradiated with UV from top, bottom and four sides of the system compared with that from only top, or top and bottom (Fig. 2D), while the total UV irradiation time was kept constant at 28 sec. These results indicate that irradiating UV light from various directions to the system forms microgels that were closer in shape to the patterns of the PDMS stencil.

It is noteworthy that the sides of the microgels are highly important surfaces in our directed assembly process. In comparison with other microscale techniques that rely on surface adhesion between different units21, microgel-directed assembly is driven by the template geometries and capillary force22. Furthermore, in order to assemble the gels, flat surfaces are necessary to stabilize each cluster prior to the secondary and tertiary crosslinking. Hence, the surface geometry of the microgels (Fig. 2B) is important to fabricate the microgel aggregates. Moreover, the photolithography process may induce cell death due to the free radicals generated by the UV irradiation23. From these points of view, the optimization of the UV direction is important for fabricating shape-controlled microgels.

Other chemically engineered hydrogels may be considered as an alternative way to obtain hydrogel blocks in order to further enhance cell viability. These include PEG hydrogels produced by Michael-type addition which does not require photoinitiator and UV irradiation24. Also, materials, such as gelatin methacrylate (GelMA) which requires shorter exposure of UV or reduced photoinitiator concentrations may be selected25.

Fabrication of assembled microgel monolayers and multi-layered constructs

Figure 3 shows images of fabricated PEGDA microgel clusters in the form of individual monolayers (Fig. 3A–D) and stacked layers (Fig. 3D–F). To assemble the microgels into an individual monolayer, the removal of excess pre-polymer was used to drive the compaction process on a hydrophilic glass surface. As the excess pre-polymer was removed, the microgels were compacted due to the capillary action of the remaining pre-polymer between the microgel units (Fig. 1A). This can be explained by the minimization of the system energy driven by the capillary forces exerted by the remaining pre-polymer26. In addition, a small agitation of the entire system provided sufficient energy to spontaneous assemble the microgel units into the monolayer with reduced local defects and overlapping. Using this approach, the formation of the uniform monolayer of at least seventy microgels was possible.

Figures 3A and B show the top-view images of microgel monolayers after assembly and photocrosslinking. Secondary photocrosslinking was used to stabilize the resulting assembly, which could be separated from the glass substrate to form a stand-alone microgel construct. The residual pre-polymer solution surrounding the individual microgels was necessary for the success of the secondary crosslinking. As can be seen in Fig. 3C, the monolayer with a uniform thickness could be formed. The building of multilayered microgel construct for fabrication of 3D construct is demonstrated in Figure 3D and E. Three individual microgel cluster layers were stacked with a small amount of the pre-polymer solution added between each layer. After removal of the excess pre-polymer solution, a thin layer of the solution remained between the adjacent microgel clusters (Fig. 3F), which made them to stick together following the tertiary photocrosslinking. The thick 3D constructs, built up layer by layer, could be used for tissue engineering applications such as building organ and other tissue-like constructs with the added benefit of controlling the cellular microenvironment in 3D.

Previously, directed assembly of cell-laden microgels was achieved by harnessing the surface tension characteristics of hydrophilic hydrogels in a two-phase oil-aqueous solution reactor15. Another recent work has created centimeter-scale cell-laden microgel assemblies at the liquid-air interfaces of a hydrophobic solution16. Although the potential advantages of directed assembly approach include the ability to direct the structure of the constructed tissue on the basis of the module geometry without the need for complicated assembly and manipulation, several factors such as capillarity, media viscosity, and hydrophobicity of the template affect the assembly of the microgel units. One of the major problems of this assembly technique is that capillary forces at the two-phase interface in solution limit the movement of the microgel units within hydrophobic oil17. In this research, we demonstrated the fabrication of multimillimeter 3D tissue constructs by stacking layers on each other.

Analysis of encapsulated cells within engineered constructs

To assess the feasibility of encapsulating cells within multilayered microgel clusters as a tool for fabricating 3D tissue constructs, NIH-3T3 cells were encapsulated in individual PEGDA microgels and their viability was evaluated by using live/dead assay (Fig. 4A). To ensure high cell viability it is important to control the photocrosslinking process, as it may induce cell damage due to the free radicals generated by the UV radiation23. In this study, we use the three step UV crosslinking to generate microgels, to stabilize individual layers of the microgels, and to stabilize the stacked layers, in which the UV irradiation time is 28, 6, and 6 sec, respectively. Therefore, we analyzed the viability of the encapsulated cells after each step. The average survival rates of NIH-3T3 cells was 94.8±3.4%, 88.6±4.0% and 80.7±1.6% for the first, secondary and tertiary crosslinking steps, respectively (Fig. 4B). As expected and similar to other published studies, the first crosslinking step for generating cell-laden microgels did not have a significant influence on the cell viability15–16. Although the viability decreased to some extent after the secondary and tertiary crosslinking steps, it still remained above 80%. The results indicate that the proposed approach in this study would be useful for fabricating 3D tissue constructs.

Generation of pores by dissolution of alginate microgels

Figure 5A shows the microscopic image of alginate microgels fabricated according to the procedure shown in Fig. 1B. The PDMS stencil filled with the alginate solution was immersed in a solution of $CaCl_2$ to crosslink the alginate polymer chains, followed by gentle collection of the gel from the stencil. Although the shape of the alginate microgels could be uniformly controlled, they shrunk about 20% after fabrication, while the shrinking ratio of the PEGDA microgel was a few percents (Fig. 5B and C). In order to adjust the size of the alginate microgels to that of the PEGDA microgels, we used a PDMS stencil having an array of hexagonal patterns of 900 μm in width for the fabrication of the alginate microgels. A microscopic image of the monolayer consisting of the PEGDA and alginate microgels is shown in Fig. 5C. As seen in this image, the size of the both microgels is almost the same and they are packed to form a uniform monolayer.

To generate pores within the layer, the assembled microgels were immersed in TPP solution that can dissolve the alginate gels. Figure 5E shows fluorescence image of the cluster consisting of the PEGDA (red) and alginate (green) microgels. As can be seen in Fig. 5F, the alginate microgel in the cluster is completely dissolved after 90 min of the TPP treatment to produce a pore. We also investigated the impact of the TPP treatment on the cell viability. There was no significant decrease in the cell viability even after 90 min of the TPP treatment (Fig. 5G). These results indicate that the alginate microgels can be used as a sacrificial material for generating pores within cell-laden microgel based constructs. In this study, we used a combination of PEGDA and alginate microgels, however other microgels such as GelMA, hydrogel comprised of modified natural ECM components25, can be used instead of the PEGDA.

Maintaining high oxygen concentration is important for cell survival in thick tissues. In most cases, cell death within the thick tissues is attributable to hypoxia rather than lack of nutrients27. To improve the supply of oxygen to 3D constructs based on cell-laden

microgels, we generated pores within the engineered structures by dissolving the alginate microgels. First, we estimated the diffusion of oxygen in the hydrogels based on Fick's diffusion laws. Because cells were distributed uniformly within the hydrogel, a spatially uniform oxygen concentration gradient was assumed. In addition, assuming a steady state system with controlled diffusion and a constant external concentration of oxygen, and constant oxygen consumption rate (OCR), the hydrogel thickness for cell survival (A [cm]) can be given as follows:

 (1)

where Do_2 is the diffusion coefficient of oxygen in the medium (cm^2/s), Co_2 is concentration of oxygen in the medium (mol/cm^3), and n is the density of cells ($cells/cm^3$). The thickness of the PEGDA microgels packed cluster that would contain a non-zero oxygen concentration was estimated to be 3.0 mm and 0.4 mm for NIH-3T3 cells and HepG2 cells, respectively, at a cell density of 2.0×10^7 cells/mL, from equation (1) with Do_2 (1.47×10^{-5} cm^2/sec)28, Co_2 (2.14×10^{-7} mol/cm^2)28, OCR values of NIH-3T3 cells (1.38×10^{-17} mol/sec/cell)29 and HepG2 cells (7.00×10^{-16} mol/sec/cell)30.

Figure 6 shows the cell viability of NIH-3T3 and HepG2 cells after 24 h in the 3D constructs consisting of the three microgel cluster layers (the thickness of each layer is 1 mm). As can be seen in Fig. 6A–C, there is no significant difference in the viability of NIH-3T3 cells among the top, middle, and bottom layer, and that the viability of each layer is approximately 80% (Fig. 6I). This result is consistent with the above prediction that the PEGDA thickness with a non-zero oxygen concentration was ~3 mm at the cell density of 2.0×10^7 cells/mL. Although this thickness of the hydrogel construct seems to be much higher than that of viable tissues without capillary networks (know as a few hundred microns)31–32, the cell density used here is not as high as that of those tissues, allowing oxygen diffusion through the hydrogel regions. In the meanwhile, most of the HepG2 cells in the middle layer did not survive (Fig. 6E) probably due to lack of oxygen supply, though the viability of the top and bottom layer is comparable with that of NIH-3T3 cells (Fig. 6D and F) and is about 70% (Fig. 6J). Figure 6G and H show fluorescence images of the HepG2 cells in the middle layer of the 3D construct having pores at the top and bottom layers. Since oxygen is accessible through the pores, the viability of the cells in and near the pores was improved. Although this result is preliminary, generating pores in the cell-laden gels could be useful to minimize hypoxia and may be potentially useful for fabricating a vascular network to supply oxygen and nutrients to the engineered tissue constructs.

Conclusion

In this report, we have demonstrated fabrication of porous 3D tissue constructs by building multilayered microgel clusters using a directed assembly technique. This technique can be used to create tightly packed multicomponent tissue-like 3D constructs with homogeneously distribution of cells. In addition, microgel blocks fabricated by sodium alginate were employed to generate porous structure within the 3D tissue-like construct. The ability to

precisely control the cell distribution and porous structure within assembled tissue-like constructs could greatly improve engineered tissue function and morphology. The proposed technique could create single layer sheet or could further be stacked to create multilayer 3D tissue constructs and this directed assembly approach can potentially become a powerful and scalable approach to generate multicomponent 3D tissue constructs in millimeter scale. Furthermore, it must be noted that the design of multicomponent 3D tissue constructs based on OCR of cell is necessary to survive cell within thick microgel 3D clusters. These techniques would be helpful for scale up of tissue engineering using biocompatible hydrogels in the future.

Acknowledgments

This paper was supported by the National Institutes of Health (DE019024; HL092836; HL099073), the National Science Foundation CAREER award (DMR0847287) and the Office of Naval Research Young Investigator award. H.K. acknowledges support from JSPS Fellowship for Research Abroad. Y.-H.J. was partially supported by the National Research Foundation of Korea Grant funded by the Korean Government [NRF-2009-352-D00107].

References

1. Langer R, Vacanti JP. Tissue engineering. Science. 1993; 260:920–926. [PubMed: 8493529]
2. Khademhosseini A, Langer R, Borenstein J, Vacanti JP. Microscale technologies for tissue engineering and biology. Proc Natl Acad Sci. 2006; 103:2480–2487. [PubMed: 16477028]
3. Mikos AG, Herring SW, Ochareon P, Elisseeff J, Lu HH, Kandel R, Schoen FJ, Toner M, Mooney D, Atala A, et al. Engineering complex tissues. Tissue Eng. 2006; 12:3307–3339. [PubMed: 17518671]
4. Bottaro DP, Liebmann-Vinson A, Heidaran MA. Molecular signaling in bioengineered tissue microenvironments. Ann N Y Acad Sci. 2002; 961:143–153. [PubMed: 12081884]
5. Mooney D, Hansen L, Vacanti J, Langer R, Farmer S, Ingber D. Switching from differentiation to growth in hepatocytes: control by extracellular matrix. J Cell Physiol. 1992; 151:497–505. [PubMed: 1295898]
6. Hollister SJ. Porous scaffold design for tissue engineering. Nat Mater. 2005; 4:518–524. [PubMed: 16003400]
7. Grande DA, Halberstadt C, Naughton G, Schwartz R, Manji R. Evaluation of matrix scaffolds for tissue engineering of articular cartilage grafts. J Biomed Mater Res. 1997; 34:211–220. [PubMed: 9029301]
8. Schreiber RE, Dunkelman NS, Naughton G, Ratcliffe A. A method for tissue engineering of cartilage by cell seeding on bioresorbable scaffolds. Ann N Y Acad Sci. 1999; 875:398–404. [PubMed: 10415586]
9. Griffith L, Naughton G. Tissue engineering--current challenges and expanding opportunities. Science. 2002; 295:1009. [PubMed: 11834815]
10. Nichol JW, Khademhosseini A. Modular tissue engineering: engineering biological tissues from the bottom up. Soft Matter. 2009; 5:1312–1319. [PubMed: 20179781]
11. McGuigan A, Sefton M. Vascularized organoid engineered by modular assembly enables blood perfusion. Proc Natl Acad Sci. 2006; 103:11461. [PubMed: 16864785]
12. Yeh J, Ling Y, Karp J, Gantz J, Chandawarkar A, Eng G, Blumling Iii J, Langer R, Khademhosseini A. Micromolding of shape-controlled, harvestable cell-laden hydrogels. Biomaterials. 2006; 27:5391–5398. [PubMed: 16828863]
13. Tsang V, Chen A, Cho L, Jadin K, Sah R, DeLong S, West J, Bhatia S. Fabrication of 3D hepatic tissues by additive photopatterning of cellular hydrogels. FASEB J. 2007; 21:790. [PubMed: 17197384]
14. Chung S, Park W, Shin S, Lee S, Kwon S. Guided and fluidic self-assembly of microstructures using railed microfluidic channels. Nat Mater. 2008; 7:581–587. [PubMed: 18552850]

15. Du YA, Lo E, Ali S, Khademhosseini A. Directed assembly of cell-laden microgels for fabrication of 3D tissue constructs. Proc Natl Acad Sci. 2008; 105:9522–9527. [PubMed: 18599452]
16. Zamanian B, Masaeli M, Nichol J, Khabiry M, Hancock M, Bae H, Khademhosseini A. Interface-directed self-assembly of cell-laden microgels. Small. 2010; 6:937–944. [PubMed: 20358531]
17. Fernandez JG, Khademhosseini A. Micro-masonry: construction of 3D structures by microscale self-assembly. Adv Mater. 2010; 22:2538–2541. [PubMed: 20440697]
18. Lin C, Lee G, Chang B, Chang G. A new fabrication process for ultra-thick microfluidic microstructures utilizing SU-8 photoresist. J Micromech Microeng. 2002; 12:590.
19. Serp D, Cantana E, Heinzen C, Von Stockar U, Marison IW. Characterization of an encapsulation device for the production of monodisperse alginate beads for cell immobilization. Biotechnol Bioeng. 2000; 70:41–53. [PubMed: 10940862]
20. Dang TT, Xu Q, Bratlie KM, O'Sullivan ES, Chen XY, Langer R, Anderson DG. Microfabrication of homogenous, asymmetric cell-laden hydrogel capsules. Biomaterials. 2009; 30:6896–6902. [PubMed: 19800116]
21. Clark, v; Tien, J.; Duffy, D.; Paul, K.; Whitesides, G. Self-assembly of 10 μm sized objects into ordered three-dimensional arrays. J Am Chem Soc. 2001; 123:7677–7682. [PubMed: 11480990]
22. Bowden N, Terfort A, Carbeck J, Whitesides G. Self-assembly of mesoscale objects into ordered two-dimensional arrays. Science. 1997; 276:233. [PubMed: 9092466]
23. Pfeifer G, You Y, Besaratinia A. Mutations induced by ultraviolet light. Mutat Res Fund Mol Mech Mutagen. 2005; 571:19–31.
24. Lutolf MP, Lauer-Fields JL, Schmoekel HG, Metters AT, Weber FE, Fields GB, Hubbell JA. Synthetic matrix metalloproteinase-sensitive hydrogels for the conduction of tissue regeneration: engineering cell-invasion characteristics. Proc Natl Acad Sci. 2003; 100:5413–5418. [PubMed: 12686696]
25. Nichol JW, Koshy ST, Bae H, Hwang CM, Yamanlar S, Khademhosseini A. Cell-laden microengineered gelatin methacrylate hydrogels. Biomaterials. 2010; 31:5536–5544. [PubMed: 20417964]
26. Scheel M, Seemann R, Brinkmann M, Di Michiel M, Sheppard A, Breidenbach B, Herminghaus S. Morphological clues to wet granular pile stability. Nat Mater. 2008; 7:189–193. [PubMed: 18264104]
27. Choi NW, Cabodi M, Held B, Gleghorn JP, Bonassar LJ, Stroock AD. Microfluidic scaffolds for tissue engineering. Nat Mater. 2007; 6:908–915. [PubMed: 17906630]
28. Provin C, Takano K, Yoshida T, Sakai Y, Fujii T, Shirakashi R. Low O2 metabolism of HepG2 cells cultured at high density in a 3D microstructured scaffold. Biomed Microdevices. 2009; 11:485–494. [PubMed: 19082898]
29. Thomas PC, Halter M, Tona A, Raghavan SR, Plant AL, Forry SP. A noninvasive thin film sensor for monitoring oxygen tension during in vitro cell culture. Anal Chem. 2009; 81:9239–9246. [PubMed: 19860390]
30. Smith MD, Smirthwaite AD, Cairns DE, Cousins RB, Gaylor JD. Techniques for measurement of oxygen consumption rates of hepatocytes during attachment and post-attachment. Int J Artif Organs. 1996; 19:36–44. [PubMed: 8641817]
31. Langer RS, Vacanti JP. Tissue engineering: the challenges ahead. Sci Am. 1999; 280:86–89. [PubMed: 10201120]
32. Shimizu T, Sekine H, Yang J, Isoi Y, Yamato M, Kikuchi A, Kobayashi E, Okano T. Polysurgery of cell sheet grafts overcomes diffusion limits to produce thick, vascularized myocardial tissues. FASEB J. 2006; 20:708–710. [PubMed: 16439619]

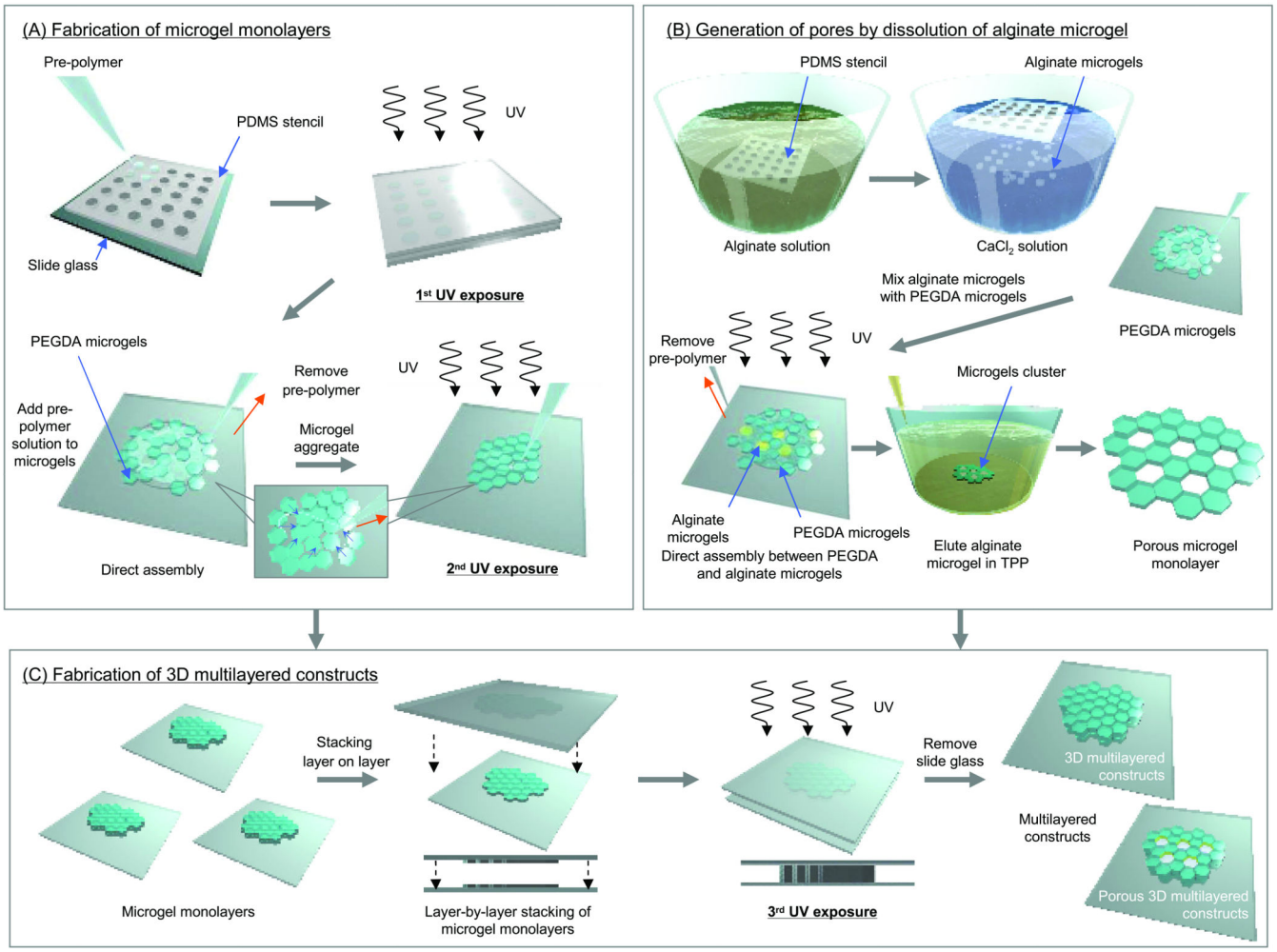

Figure 1.

Schematic diagram of the microgel assembly process. (A) PEGDA microgels and microgel monolayer were fabricated by photolithography. To assemble the microgels into a monolayer, the gels were placed on a slide and the excess pre-polymer solution was removed by a pipette and an absorbent material. Subsequently, the microgels in the monolayer were crosslinked by exposure to light. (B) To generate of pores in microgel monolayer, alginate microgels were fabricated as sacrificial templates using a PDMS stencil. The suspension of alginate was immediately poured into the hexagonal patterned PDMS stencil and excess alginate was removed by gently wiping the stencil. The stencil was immediately immersed in a $CaCl_2$ solution which crosslinks the alginate polymer chains into a hydrogel. After PEGDA and alginate microgels were mixed on the glass substrate, pre-polymer solution was removed to assemble the microgels into a monolayer. The resulting monolayer was subsequently exposed to light to crosslink the PEGDA microgels to each other. To elute sodium alginate microgel units, the assembled microgel were immersed in TPP solution. (C) To fabricate the 3D constructs, microgel monolayer units were stacked in a layer by layer manner on a glass slide, and pre-polymer solution was added between each

layer. To stabilize the stacked layers, the entire construct was exposed to a tertiary crosslinking step.

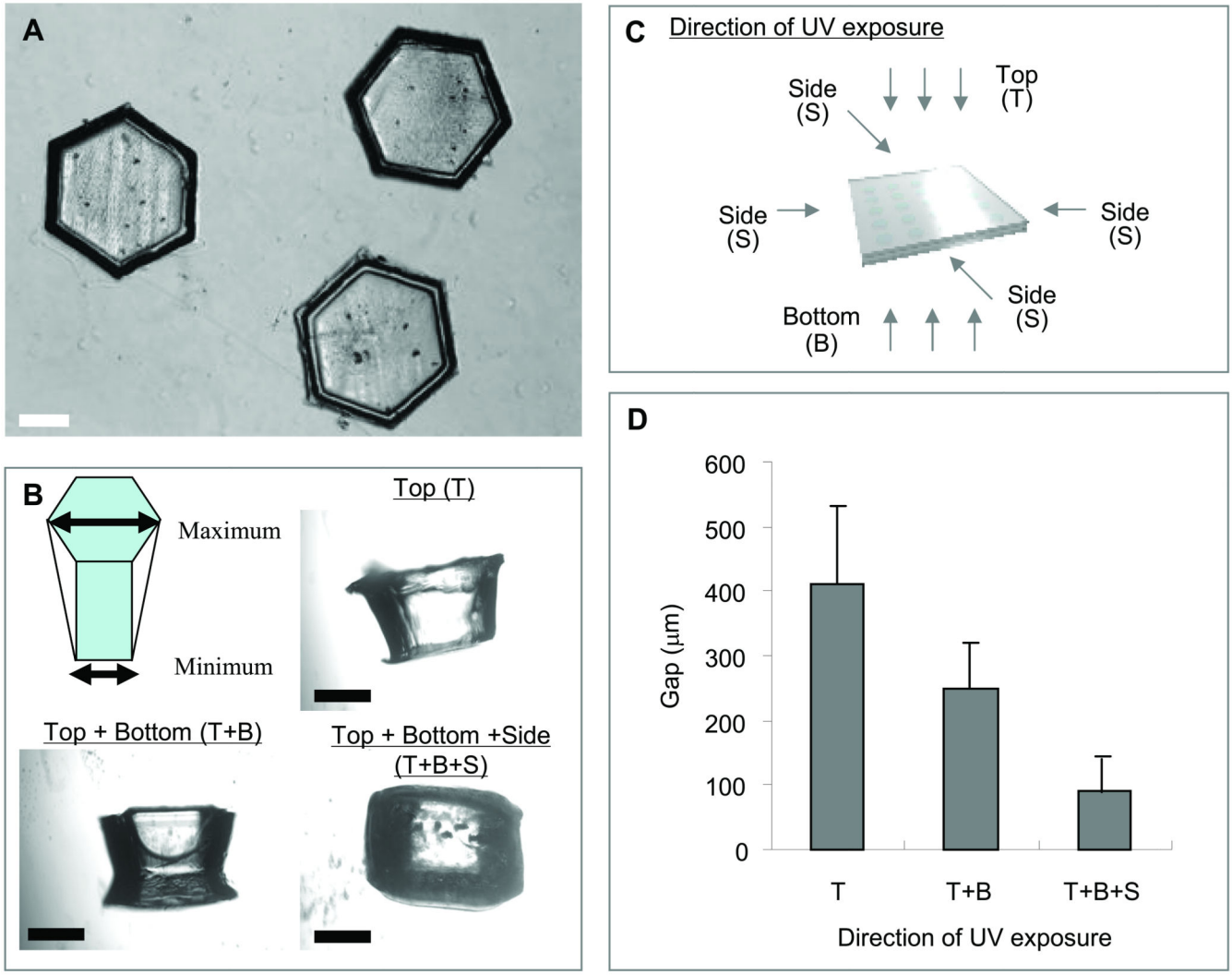

Figure 2.

Microscopic images of (A) top and (B) side of photocrosslinked PEGDA microgel units. (C) Schematic diagram of microgel unit fabrication process with the UV light exposure from various directions. (D) The gap between maximum and minimum width of a microgel. While the total UV irradiation time was 28 sec, the UV was irradiated from only top (28 sec), top (14 sec) and bottom (14 sec), top (10 sec) and bottom (10 sec) and 4 sides (2 sec per each side). Each value represents the mean ± S.D. (n=3). [Scale bars = 500 μm]

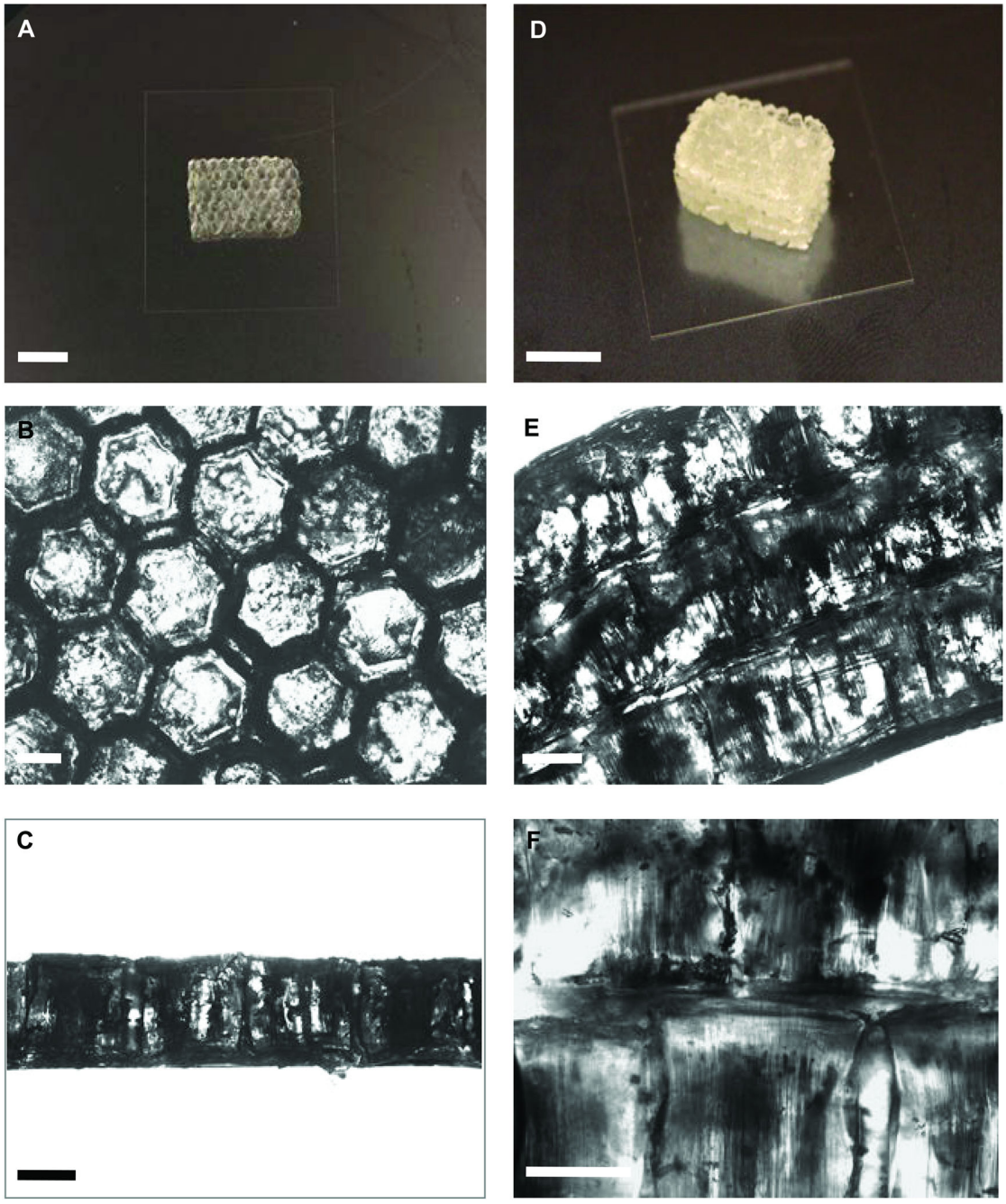

Figure 3.

(A) Photograph of assembled PEGDA microgel monolayer after secondary crosslinking. Bar in A is 1 cm. Microscope images of (B) top-view and (C) side-view of microgel monolayers. Bars in B and C are 500 μm. (D) Photograph of multilayer PEGDA microgel assemblies after a tertiary crosslinking. Bar in D is 1 cm. Microscope images of (E) side-view of multilayered structure and (F) the junction between adjacent monolayers after tertiary crosslinking. Bars in E and F are 500 μm

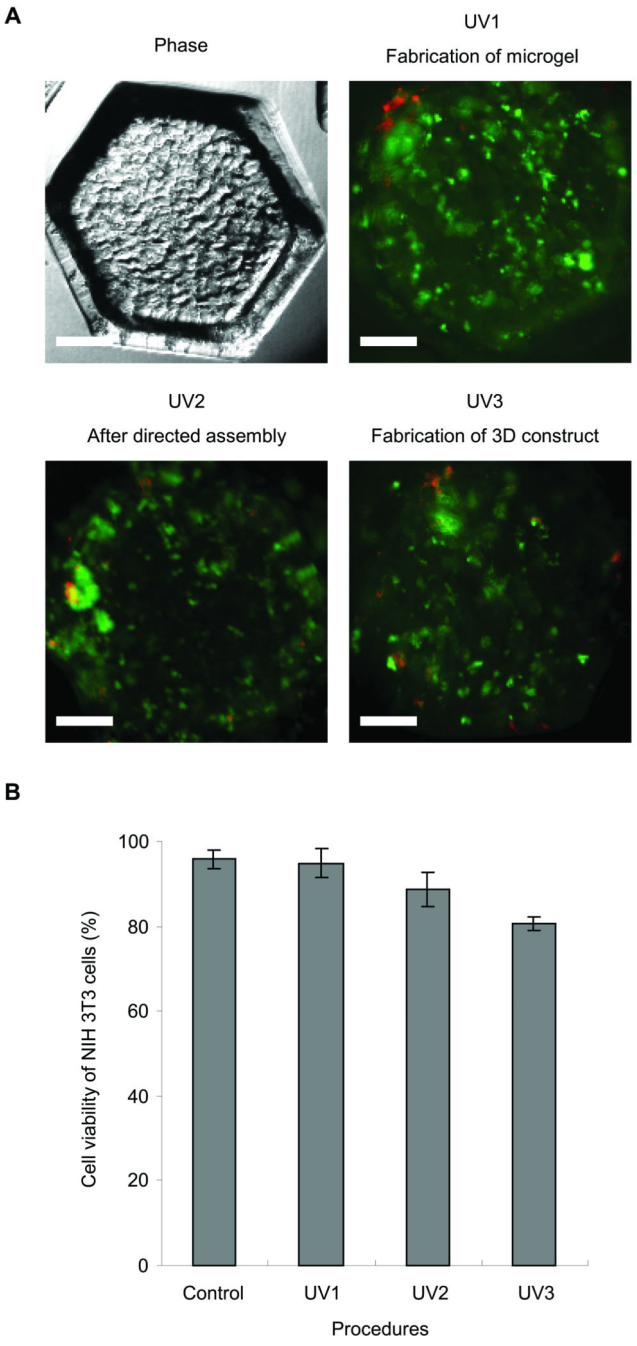

Figure 4.

Cell viability analysis at a density of 1×10^6 cells / mL as a function of steps in the assembly procedure. (A) Phase-contrast and fluorescence images of cell-laden (NIH-3T3) microgels after first (28 sec), second (6 sec) and third (6 sec) crosslinking steps. (B) Quantified cell viability after each step in the procedure to fabricate microgels cluster. Each value represents the mean ± S.D. (n=5). Scale bars = 250μm

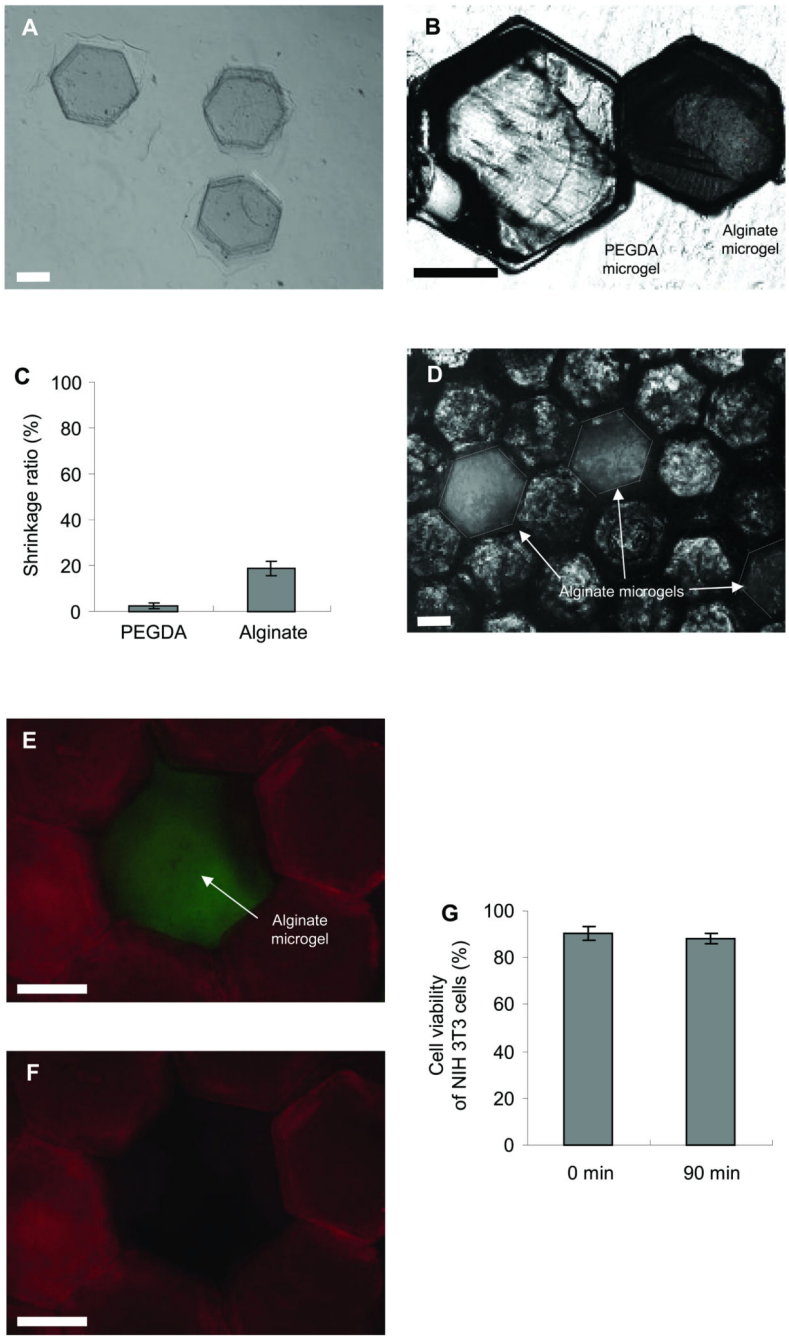

Figure 5.

Light and fluorescent microscopic images of PEGDA and alginate microgels. (A) Phase-contrast of alginate microgels in $CaCl_2$ solution. (B) Image of a PEGDA and alginate microgel after fabrication by using a 900 μm PDMS stencil. As it can be seen alginate microgels had a significant degree of shrinking. (C) Shrinkage ratio of PEGDA and alginate microgels after fabrication. Each value represents the mean ± S.D. (n=10). (D) A layer of microgels containing PEGDA and alginate microgels. Images of a microgel monolayer made from PEGDA and alginate microgels in TPP 22 solution at (E) 0 min and (F) 90 min.

(G) NIH-3T3 cell viability analysis as a function of steps in the dissolution of alginate microgels. Each value represents the mean ± S.D. (n=5). Bars = 500 μm.

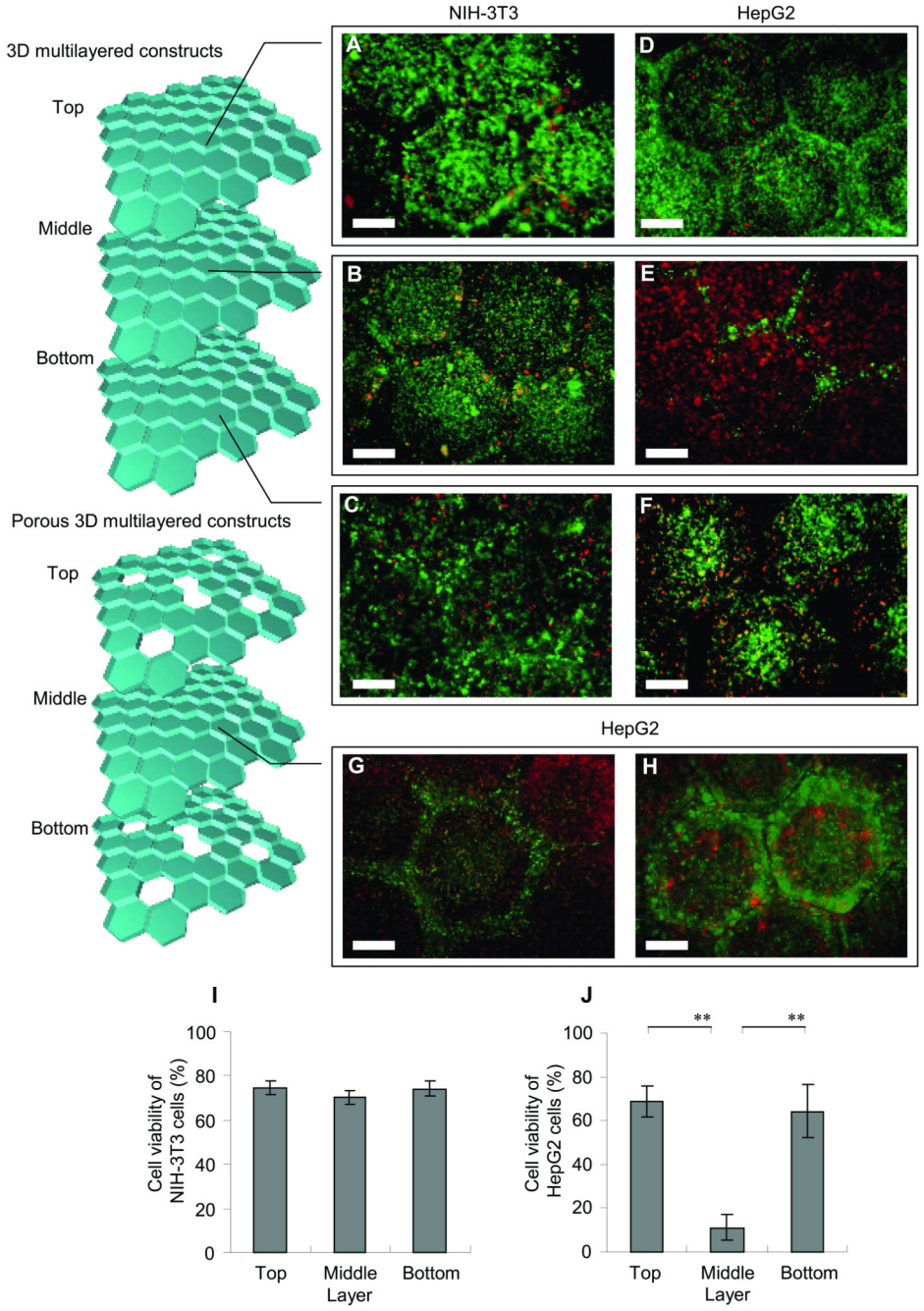

Figure 6.

Cell viability analysis in 3D microgel multilayer constructs after 24 h at a density of 2×10^7 cells / mL. Images of cell viability of NIH-3T3 in (A) top, (B) middle and (C) bottom of microgel monolayers and HepG2 cells in (D) top, (E) middle without pores and with pores (G and H) to supply nutrients and oxygen, and (F) bottom of microgel monolayers. Quantified cell viability of (I) NIH-3T3 and (J) HepG2 cells after 24 h. Each value

represents the mean ± S.D. (n=5). The data for HepG2 cells in top or bottom clusters and middle cluster (**) gave a p-value < 0.01. Bars = 500 μm